

Endpoint Detection Using Optical Emission Spectroscopy in TSV Fabrication

Ja Myung Gu^{1,2}, Paragkumar A. Thadesar², Ashish Dembla²,
Sang Jeen Hong¹, Muhannad S. Bakir², and Gary S. May^{2*}

¹Department of Electronic Engineering, Myongji University, Korea

²School of Electrical and Computer Engineering, Georgia Institute of Technology, USA
gary.may@coe.gatech.edu

ABSTRACT

A hybrid partial least squares-support vector machine (PLS-SVM) model of optical emission spectroscopy data is proposed and successfully demonstrated to predict the endpoint detection of through silicon vias (TSVs) etched using the Bosch process. Accurate results are shown for TSVs with diameters of 80 μm and 25 μm .

INTRODUCTION

System interconnections have emerged as a critical bottleneck to the performance of modern computing systems. To alleviate this issue, three-dimensional (3D) and 2.5 dimensional (2.5D) integration of chips have been widely explored [1]. Through silicon vias (TSVs) are a key technology enabler for 3D and 2.5D semiconductor device integration. For TSV fabrication, either blind vias can be etched first in silicon followed by back side silicon polishing or vias can be etched through the entire thickness of silicon. The latter approach alleviates the requirement for silicon polishing after via etch and is the focus of this paper.

While we emphasize TSVs in this paper, the results of the research under consideration can be used in various applications, including MEMS, microfluidic, electronic device fabrication, etc. TSV etching is primarily performed using the Bosch process with alternating etch and passivation cycles. SF_6 is used as the reactive etch gas, and C_4F_8 is used for fluorocarbon sidewall passivation. During via etching, run-to-run variation in etch rate can be observed due to changes in process conditions, leading to over or under etching for a fixed number of process cycles. An example of 300 μm tall over-etched vias is shown in Fig. 1.

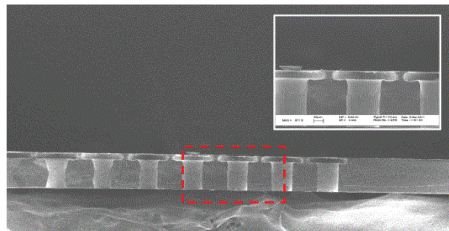


Fig. 1 Over etched 120 μm diameter TSVs, inset shows magnified image.

In order to obtain control over critical dimensions, it is important to accurately detect the endpoint during dry etching of TSVs. Using conventional endpoint detection techniques [2], it is difficult to predict the endpoint for TSVs etched using the Bosch process because of the multiple cycles of etch and passivation. To alleviate this

challenge, a hybrid partial least squares-support vector machine (PLS-SVM) model using optical emission spectroscopy (OES) data is employed and successfully demonstrated for TSVs with diameters of 80 μm and 25 μm .

The OES technique is used to monitor *in-situ* plasma process conditions during silicon etching and involves measuring optical emission of the plasma in the UV/VIS (200 nm to 1000 nm) range with different wavelengths corresponding to different elements and radicals [3]. Specific positive ion species and radicals corresponding to their optical emission wavelengths were observed, and their optical emission intensities were monitored. Data analysis was performed using PLS [4] and SVM [5] to establish predictive endpoint detection (EPD) models for TSVs.

EXPERIMENTAL SETUP AND SAMPLE PREPARATION

TSV etching was performed in an STS inductively coupled plasma (ICP) system using Bosch process with an OES system installed on top of process chamber (Fig. 2).

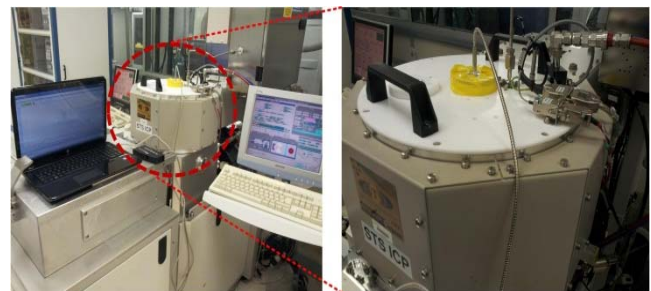


Fig. 2 OES setup with sensor mounted on top of ICP etching tool process chamber (closer image shown on right)

To fabricate the TSVs, a silicon dioxide etch-stop layer was first deposited on one surface of a 4-inch silicon wafer, followed by photolithography to form a photoresist etch mask for silicon etching. To alleviate wafer-to-wafer thickness variation in the sample, TSV etching was performed on one half of the wafer first while keeping other half of the wafer covered. Once the etching of the first half was completed, the second half was etched based on the EPD prediction to confirm the accuracy of the model.

RESULTS AND DISCUSSION

The proposed hybrid PLS-SVM model consists of 6 steps, as shown in Fig. 3.

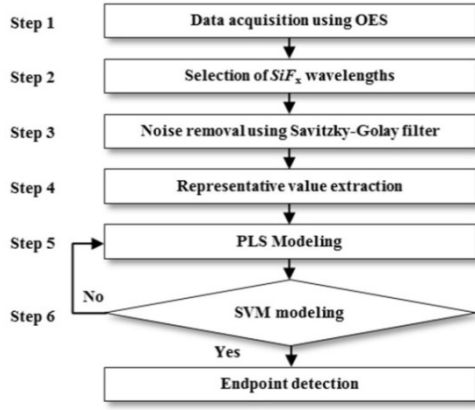


Fig. 3 Flowchart of the proposed hybrid PLS-SVM model

A. Steps 1 to 4: Feature data preprocessing

The most significant by-products in silicon etching with SF_6 plasma are SiF_x radicals (Fig. 4). During the Bosch process, multiple optical emission wavelengths related to SiF_x group were identified, and they showed reasonable emission intensity changes around TSV endpoint.

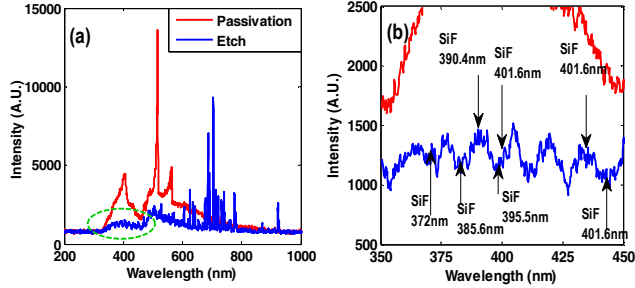


Fig. 4 (a) Passivation and etch step spectra for silicon etch process; the plasma emission spectra of both steps are dramatically different. (b) Magnified image (green circle) of (a); selected SiF_x species in etch step during silicon etching.

To extract a meaningful endpoint signal during the Bosch process, the SiF_x OES signals were filtered using a Savitzky-Golay smoothing filter [6] to eliminate noise from the SiF_x related peaks, as shown in Fig. 5(a). The general equation of the simplified least-squares convolution for the acquired OES raw filtered data is as follows:

$$Y_j^* = \frac{\sum_{i=-m}^{i=m} C_i Y_{j+i}}{N} \quad (1)$$

where Y is the original OES data, Y^* is the resultant OES data, C_i is the coefficient for the i^{th} observation of the filter (smoothing window), and N is the number of convoluting integers, which is equal to the smoothing window size ($2m + 1$). The index j is the running index of the original ordinate data table. The smoothing array (filter size) consists of $2m+1$ points, where m is the half-width of the smoothing window. When the filter is applied to SiF_x wavelength smoothing, there are two parameters that must

be determined. The first parameter is m , the half-width of the smoothing window. Usually, a larger value of m produces a smoother result at the expense of flattening sharp peaks. The second parameter is an integer C_i specifying the degree of the smoothing polynomial, which is typically set in a range of 2 to 4. After the SiF_x wavelengths were smoothed, the intensities were integrated over etch cycles to generate mean representative intensity values, as shown in Fig. 5(b).

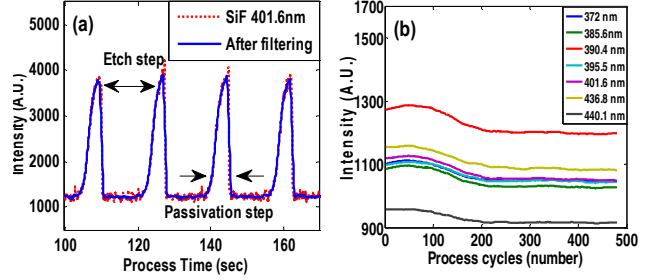


Fig. 5 (a) Filtered SiF_x intensity using the Savitzky-Golay smoothing filter (b) Mean integrated values of SiF_x intensity during etch cycles.

B. Step 5: PLS modeling for creating endpoint signal

Partial least squares (PLS) regression based on principal component analysis (PCA) is employed in many fields of chemistry-analytical, physical, clinical chemistry and industrial process control. PLS is an extension of the NIPALS algorithm [7]. The main idea of PLS is to successively select directions of variation in the input data matrix X that maximize the output variation that can be predicted. Thus, the PLS decomposition consists of outer relations (X and Y individually) $X=TP^T$ and $Y=UQ^T$ and an inner relationship linking X and Y , $U=TB$ with the final regression model given by $Y=TBQ^T$. In the NIPALS implementation of PLS, the recursive computation of the columns of T and U is done simultaneously with information exchanged between them at each step to ensure optimal alignment. The input matrix is comprised of the generated mean representative value form seven SiF_x wavelengths, while the output matrix Y is constructed by the product of raw spectrum data and signal vectors around the endpoint. Fig. 6 shows the endpoint signal generated using PLS for TSVs with a diameter of 80 μm . As shown, an enhanced endpoint signal was obtained, and the difference between before and after the expected endpoint (blue circle in Fig. 6) is significantly increased.

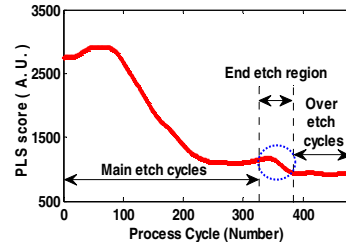


Fig. 6 The generated endpoint signal in 80 μm diameter TSVs from the first run of back-to-back etching using a PLS

C. Step 6: SVM modeling for detecting endpoint

Support vector machines (SVM) are a machine learning method based on the foundation of statistical learning theory. A SVM performs classification by constructing an n -dimensional hyper-plane that optimally separates the etch data into two classes (before and after endpoint). The data points forming the optimal hyper-plane are called support vectors (Fig. 7).

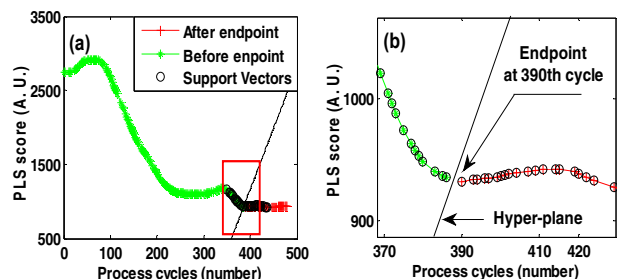


Fig. 7 (a) Endpoint prediction by applying SVM and (b) Magnified image (red square) of (a); Endpoint detection at 390th cycle.

D. PLS-SVM model verification

The hybrid PLS-SVM model was verified by back-to-back etching of 80 μm and 25 μm diameter TSVs. The endpoint obtained from the first half of the wafer was applied to accurately predict the endpoint of the second half of the wafer, as described previously. Table 1 shows the results of back-to-back etching of 80 μm and 25 μm TSVs. The etch result are shown in Fig. 8 and Fig. 9.

Table 1. The sample for endpoint detection

TSV Diam. (μm)	Wafer Half	Process Cycle	Average diameter for 100 vias (μm)		Variations between the maximum and the minimum diameters (μm)	
			Top	Bottom	Top	Bottom
80	1 st	480	84.72	122.85	5.96	12.21
	2 nd	390	83.11	79.54	3.98	6.54
25	1 st	650	29.61	48.39	1.84	5.43
	2 nd	624	28.87	28.20	1.5	3.81

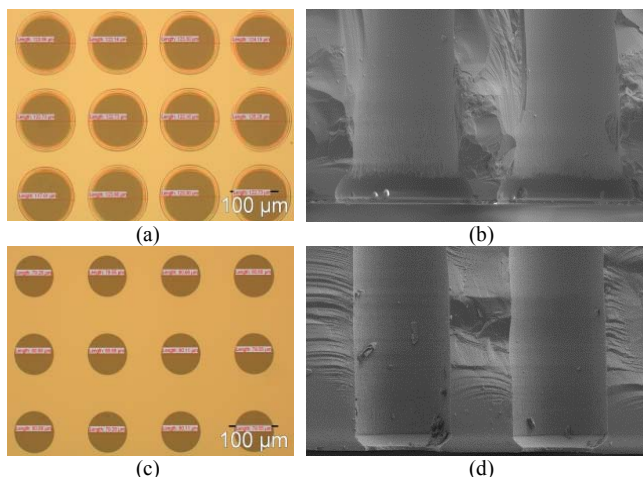


Fig. 8 (a) Bottom view;(b) Cross-section view of 80 μm diameter TSVs after etching the first half of a wafer for 480 cycles; (c) Bottom view; and (d) Cross-section view of 80 μm diameter TSVs after etching the second half of a wafer for 390 cycles as predicted endpoint.

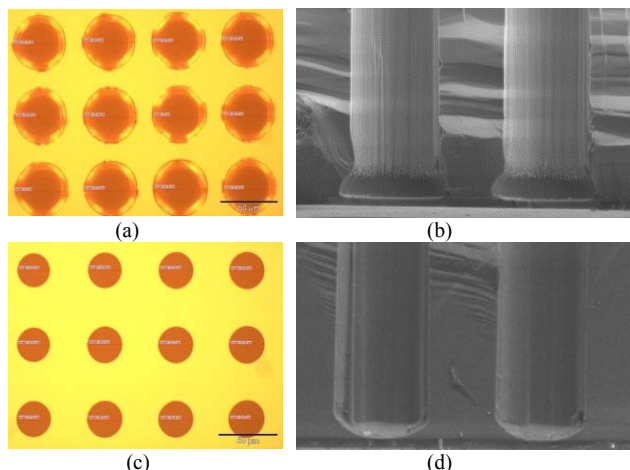


Fig. 9 (a) Bottom view;(b) Cross-section view of 25 μm diameter TSVs after etching the first half of a wafer for 650 cycles; (c) Bottom view; and (d) cross-section view of 25 μm diameter TSVs after etching the second half of a wafer for 624 cycles as predicted endpoint.

CONCLUSIONS

A hybrid PLS-SVM model using OES is proposed and successfully demonstrated for the Bosch process etching of 80 μm and 25 μm diameter TSVs. A minor difference (1.61 μm in 80 μm TSV, 0.74 μm in 25 μm TSV) between the top and bottom diameters of the TSVs was observed after etching, but overall the PLS-SVM based endpoint predictive model demonstrates good accuracy in TSV fabrication.

REFERENCES

- [1] J. U. Knickerbocker, J.U. Knickerbocker, P.S. Andry, E. Colgan, B. Dang, T. Dickson, X. Gu, C. Haymes, C. Jahnes, Y. Liu, J. Maria, R.J. Polastre, C.K. Tsang, L. Turlapati, B.C. Webb, L. Wiggins and S.L. Wright "2.5D and 3D technology challenges and test vehicle demonstrations," in *Proc. 62nd IEEE Electronic Components and Technology Conference (ECTC)*, pp. 1068 - 1076, 2012
- [2] H. Yue, S. J. Qin, J. Wiseman, and A. Toprac, "Plasma etching endpoint detection using multiple wavelengths for small open-area wafers," *Journal of Vacuum Science & Technology A: Vacuum, Surfaces, and Films*, vol. 19, no. 1, pp. 66–75, Jan/Feb 2001.
- [3] D.A. White, B.E. Goodlin, A.E. Gower, D.S. Boning, H. Chen, H.H. Sawin, T.J. Dalton, "Low open-area endpoint detection using a PCA-based T2 statistic and Q statistic on optical emission spectroscopy measurements," *IEEE Transactions on Semiconductor Manufacturing*, 13(2): pp. 193-207, 2000.
- [4] W. Lindberg, J.-A. Persson and S. Wold, "Partial Least-Squares Method for Spectrofluorimetric Analysis of Mixtures of Humic Acid and Lignin Sulfonate," *Journal of Analytical Chemistry*, vol. 55, pp. 6, 1983.
- [5] J. A. K. Suykens, J. Vandewalle, "Least Squares Support Vector Machine Classifiers," *Neural Processing Letters*, vol. 9, no. 3, pp. 293-300, 1999.
- [6] J. Serafinczuk, J. Pietrucha, G. Schroeder, and T. P. Gotszalk, "Thin Film Thickness Determination Using X-Ray Reflectivity and Savitzky-Golay Algorithm," *Optica Applicata*, vol. 41, no. 2, pp. 315-322, 2011.
- [7] P. Geladi and B. R. Kowalski, "Partial Least-Squares Regression: A Tutorial," *Analytica Chimica Acta*, vol. 185, pp. 17, 1986.